Electronic Supplementary Information for Analyst
This journal is © The Royal Society of Chemistry 2020

Fabrication and Application of a Novel Electrochemical Biosensor Based on Mesoporous Carbon Sphere@UiO-66-NH_2/Lac Complex Enzyme for Tetracycline Detection

Xiaomin Zhong[a], Fang Wang[b], Jinhua Piao[a,*], Yitao Chen[c]

a. *School of Food Science and Engineering, South China University of Technology, Guangzhou 510641, Guangdong, PR China*
b. *School of Environmental Engineering and Chemistry, Luoyang Institute of Science and Technology, Luoyang, 471023, PR China*
c. *School of Life and Environmental Science, Guilin University of Electronic Technology, Guilin, 541004, Guangxi, PR China*

* Corresponding author. Tel: 86-20-87113849; Fax: 86-20-87113849.
E-mail address: jhpiao@scut.edu.cn (J. Piao)

Table of contents

Supplementary information

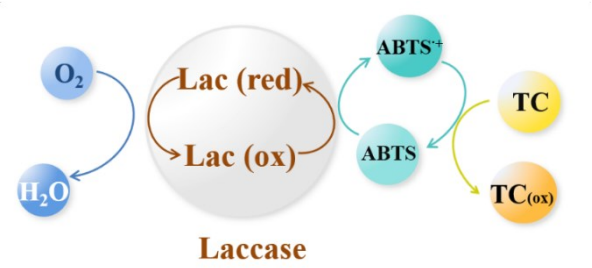

Scheme S1 Schematic illustration of tetracycline oxidation mechanism of the MCS@UiO-66-NH_2/Lac/ABTS/CHIT/GCE tetracycline biosensor.[S1]

Experimental section

Chemicals and reagents

Sodium hydroxide (NaOH, 96%), hydrochloric acid (HCl, 36%-38%), sodium acetate (NaAc, 99%), acetic acid (HAc, 99.5%), soluble starch, ammonium hydroxide ($NH_3 \cdot H_2O$, 25%-28%), potassium ferricyanide (99.5%), potassium ferrocyanide (99.5%) and potassium chloride (99.5%) were purchased from Tianjin Damao Chemical Reagent Factory (Tianjin, China).

Synthesis of mesoporous carbon sphere (MCS)

The preparation process of MCS is showed in Scheme S2†.[S2,S3] Starch (10.5 g) was dissolved in a mixed solution (70 mL) which consisted of deionized water and ethanol solution in the volume ratio of 1:1, and then $NH_3 \cdot H_2O$ (1 mL) and TEOS (2 mL) were added in sequence under stirring. Subsequently, the above solution was transferred to a 100 mL Teflon-lined stainless-steel autoclave to react at 190 ℃ for 12 h. After washed by water and ethanol, the samples were heated in a tubular furnace at 800 °C for 3 h under nitrogen atmosphere. Then the MCS material was obtained after the above product was etched by 1M NaOH at 70 ℃. Average size and size distribution of MCS

and MCS@UiO-66-NH_2 composite were analyzed using the ImageJ software.

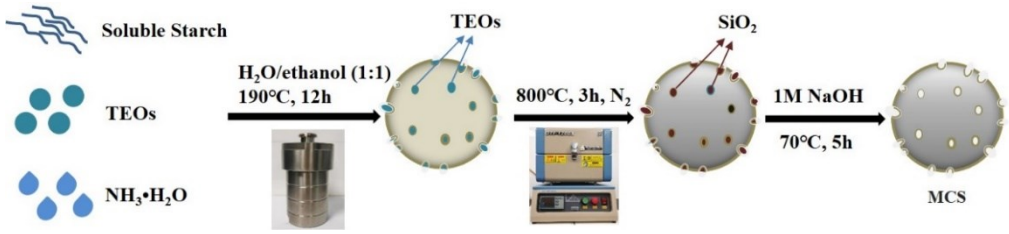

Scheme S2 Schematic illustration of the synthesis process of MCS.

Synthesis of MCS@UiO-66-NH_2 composite

The synthesis process of the MCS/UiO-66-NH_2 composite is display in Scheme S3†. $ZrCl_4$ (125 mg) was dissolved in the mixture of DMF (5 mL) and HCl (1 mL) by using ultrasound for 15 minutes. Then, benzoic acid (1.96 g), NH_2-BDC (134 mg), DMF (10 mL) were added to the mixture and dispersed by ultrasound for 10 minutes. Next, the as-prepared MCS (72 mg) was added in the mixture. Subsequently, the mixture was heated in 80 ℃ water bath for 2 h under stirring and transferred to a 100 mL Teflon-lined stainless-steel autoclave at 80 ℃ for 24 h. After cooled to room temperature, the sample was centrifuged and washed with DMF/ethanol for several times. The final MCS@UiO-66-NH_2 composite was obtained by vacuum drying at 60 ℃ for 24 h. As a contrast, UiO-66 and UiO-66-NH_2 were also prepared using the same method.

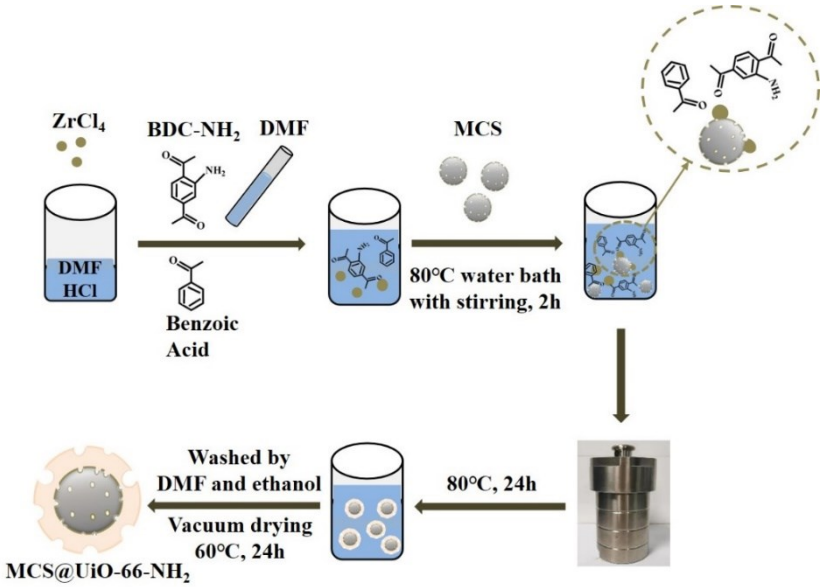

Scheme S3 Schematic illustration of the synthesis process of the MCS/UiO-66-NH_2 composite.

Analysis of enzyme loading on the MCS@UiO-66-NH_2 composite

The MCS@UiO-66-NH_2/Lac complex enzyme were prepared by adsorption method. The synthesized MCS@UiO-66-NH_2 composites (20 mg) were dispersed in 20 mL laccase solution of different concentration (laccase in 0.1 M HAc-NaAc buffer solution, pH=6) by stirring to form uniform mixture, then incubated at 4 ℃ for 12 h. Enzyme loading on MCS@UiO-66-NH_2, expressed in mg g^{-1}, was determined by the Bradford method.[S4] It is a common method to determine the amount of immobilized enzyme measuring the difference between the initial amount of laccase and the final laccase concentration in the mixture after immobilization. Besides, Coomassie Brilliant Blue G-250 solutions were used as standards (0-0.8 mg mL^{-1}) to plot a calibration curve. The enzyme concentration was diluted 10 times and was determined with UV−vis spectrophotometry (UV-5000, Shanghai Yuanxi instrument Company) by measuring the absorbance at 595 nm. Enzyme loading was calculated with the following equation:

$$\text{enzyme loading } (\text{mg}\cdot\text{g}^{-1}) = \frac{(C_1 - C_0)V}{M}$$

where C_1 is the final laccase concentration after immobilization (mg·mL^{-1}), C_0 is the initial laccase concentration (mg mL^{-1}), V is the enzyme volume (mL) and M is the mass of support (MCS@UiO-66-NH_2) (g).

Results and discussion section

FT-IR analysis

The FTIR spectra were characterized to further prove chemical structure of as-prepared UiO-66, UiO-66-NH_2 and MCS@UiO-66-NH_2 composite. As shown in Fig. S1†, three samples all display several peaks at 762, 746, 724, 665, 570 and 479 cm^{-1}, corresponding to the mixture of OH and CH bending with Zr-O vibrations.[S5] The peaks of 1380 and 1550 cm^{-1} are Zr−OH vibrations.[S6] Compared with the UiO-66 (Fig. S1A†(a)), a new peak appears at 1257 cm^{-1} while the intensity of the peak of 1562 cm^{-1} is also increase obviously in the spectra of the UiO-66-NH_2 (Fig. S1A†(b)) and MCS/UiO-66-NH_2 composite (Fig. S1A†(c)). The peaks at 1562 cm^{-1} and 1257 cm^{-1} are related to N–H bending vibration and C–N stretching. Furthermore, the peaks of the

symmetric and asymmetric N−H vibration at 3458 cm^{-1} and 3427 cm^{-1} prove a successful functionalization of amine (Fig. S1B†).[S7] Considering the above information and the results of XRD measurements (Fig. 1), it can be verified that the MCS@UiO-66-NH_2 composite was successfully synthesized.

Enzyme loading on MCS@UiO-66-NH_2 composite analysis

Enzyme loading on the MCS@UiO-66-NH_2 composite was evaluated to investigate the immobilization capacity of prepared composites. In general, enzyme loading increased with increasing of laccase solution concentration (Fig. S3†). The laccase loading increased to 155.08 mg g^{-1} when the initial concentration of laccase solution was 5 mg·mL^{-1}. However, the enzyme loading went to be flat and even a slight decreased when the laccase concentration was over 5 mg mL^{-1}. The excessive laccase would lead to the crowding or agglomeration of enzyme and may hinder its immobilization onto the composite.[S8] Similar phenomenon was also reported by Chao et al. in the study of improvement of laccase immobilization on halloysite nanotubes.[S9] Therefore, the laccase loading on MCS@UiO-66-NH_2 composite reached a maximum value of 155.08 mg g^{-1} at the laccase solution concentration of 5 mg mL^{-1}.

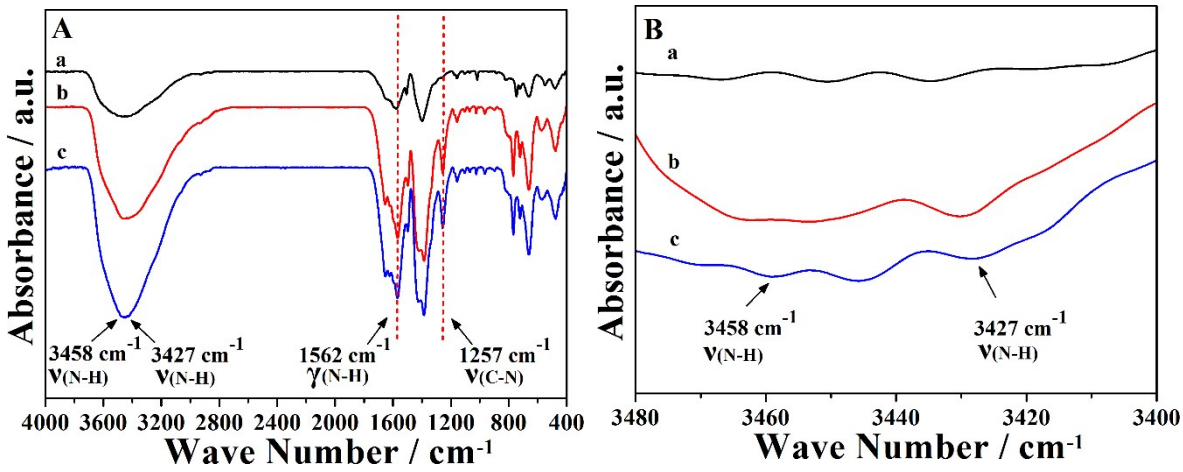

Fig. S1 (A) FT-IR spectra of the as-prepared materials: (a) UiO-66, (b) UiO-66-NH_2 and (c) MCS@UiO-66-NH_2. (B) Partial enlarged details of (A).

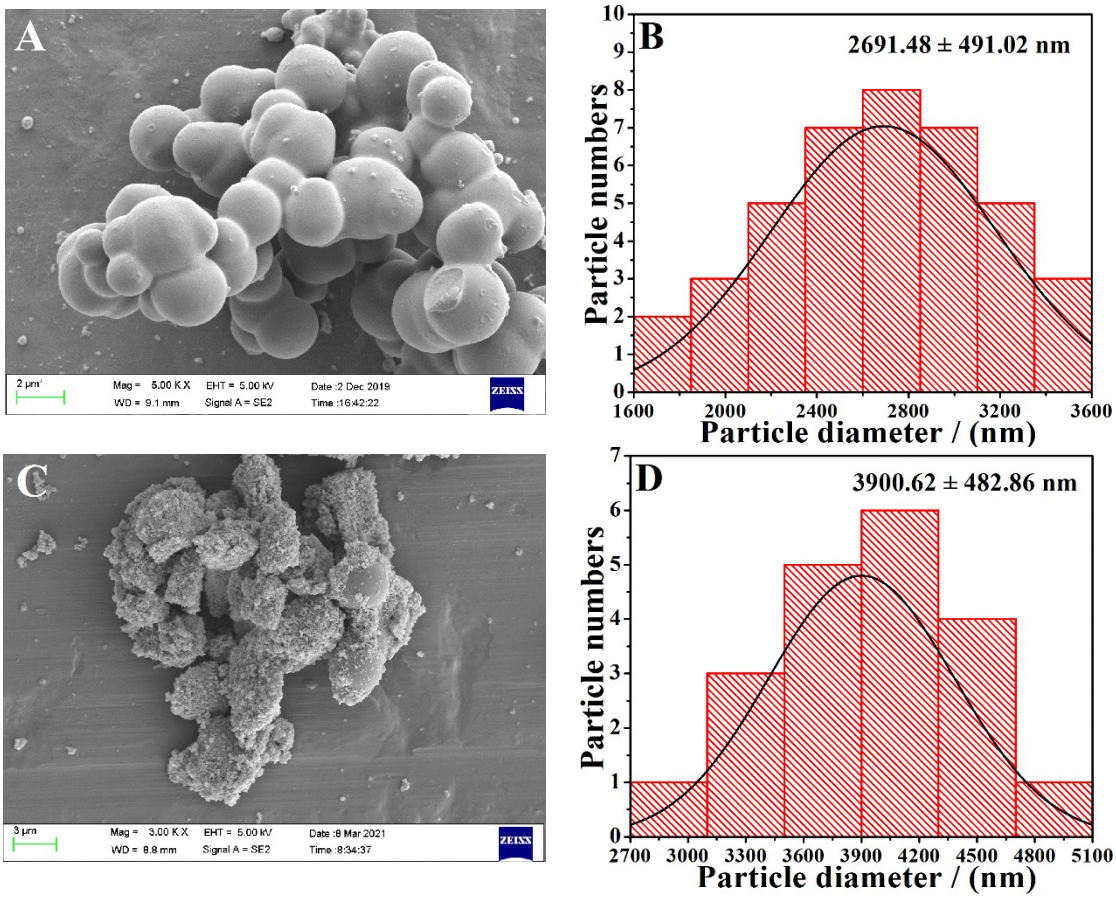

Fig. S2 (A) SEM image of MCS, (B) particle size distribution histogram obtained from SEM image (A), (C) SEM image of MCS@UiO-66-NH_2, (D) particle size distribution histogram obtained from SEM image (C).

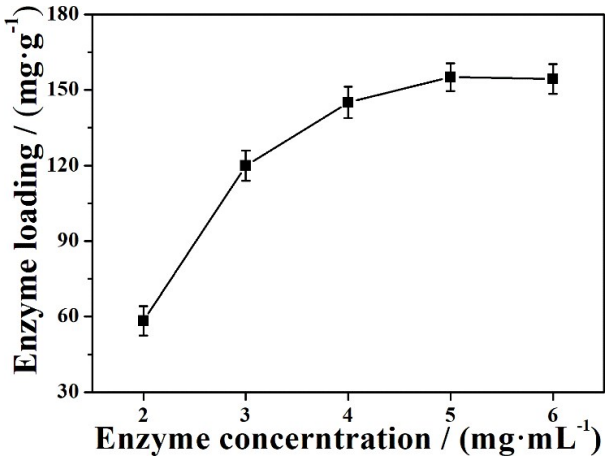

Fig. S3 Effect of the initial laccase solution concentration on the laccase loading on MCS@UiO-66-NH_2 composite

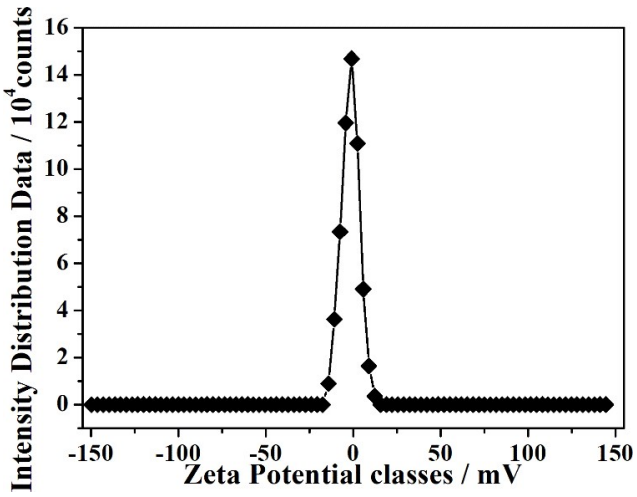

Fig. S4 Zeta-potential of MCS@UiO-66-NH_2 at the immobilization pH of 6.0.

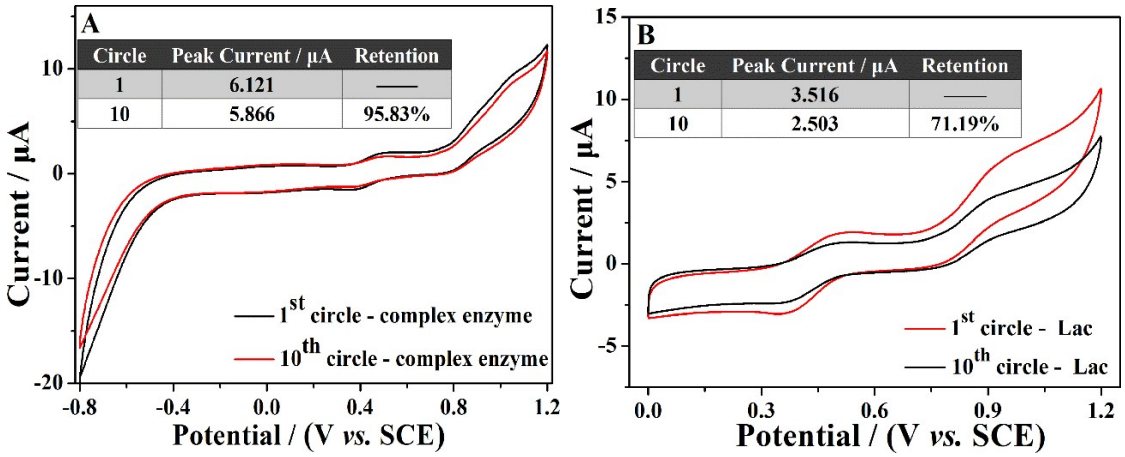

Fig. S5 Stability of as-prepared biosensors: (A) MCS/UiO-66-NH_2/Lac/ABTS/CHIT/GCE, (B) Lac/ABTS/CHIT/GCE.

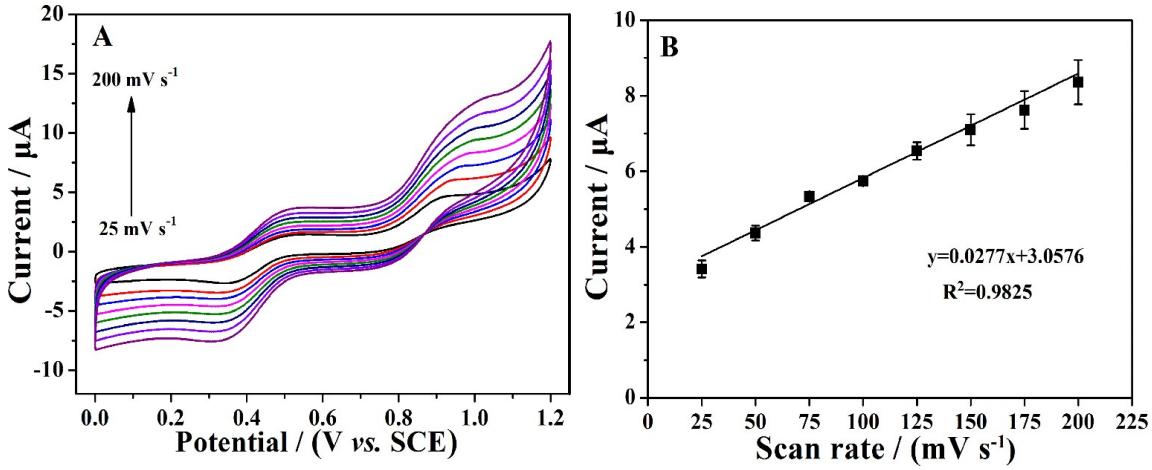

Fig. S6 (A) CVs of MCS@ UiO-66-NH_2/Lac/ABTS/CHIT/GCE biosensor measured at scan rates range 25-200 mV s^{-1}. (B) Plots of the peak current *vs*. scan rate.

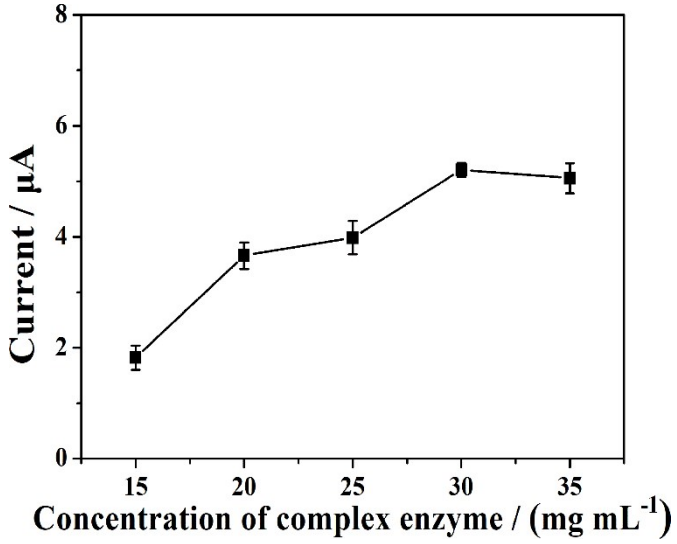

Fig. S7 Effect of the concentration of the MCS@UiO-66-NH_2/Lac complex enzyme on the response current of the MCS@UiO-66-NH_2/Lac/ABTS/CHIT/GCE biosensor.

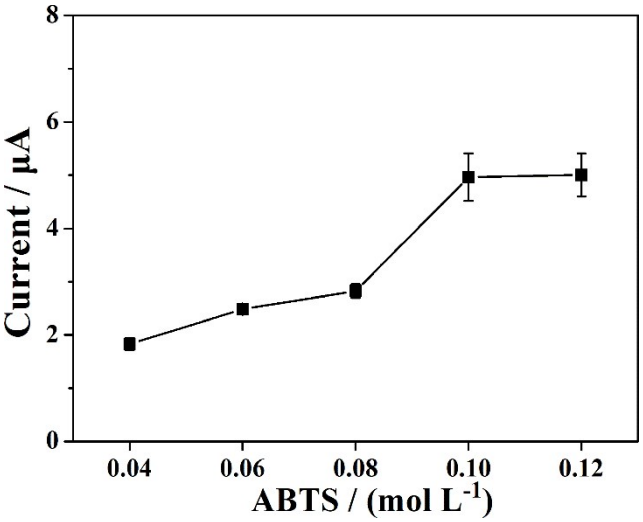

Fig. S8 Effect of the concentration of ABTS on the response current of the MCS@UiO-66-NH_2/Lac/ABTS/CHIT/GCE biosensor.

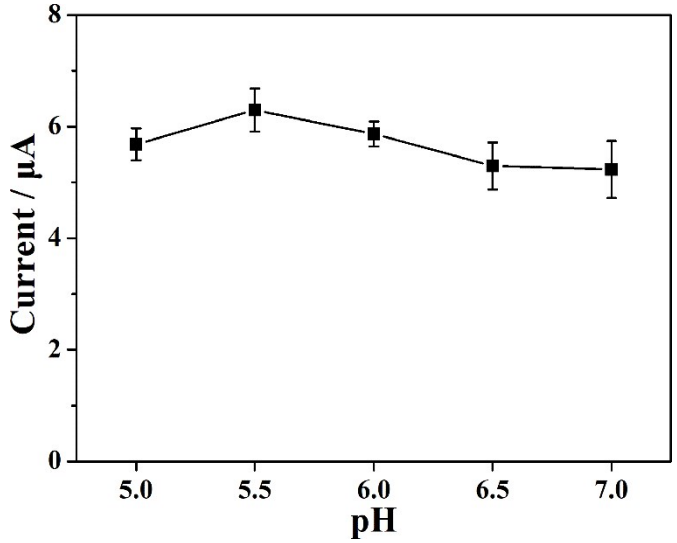

Fig. S9 Effect of the pH of HAc-NaAc suffer solution on the response current of the MCS@UiO-66-NH_2/Lac/ABTS/CHIT/GCE biosensor.

Table S1 The BET surface areas and pore parameters of the prepared materials

Materials	BET Surface Area ($m^2\ g^{-1}$)	BJH Average Pore Diameter (nm)	Pore Volume ($cm^3\ g^{-1}$)
UiO-66-NH_2	773.37	2.47	0.45
MCS	18.96	7.04	0.05
MCS@UIO-66-NH_2 composites	700.89	17.37	0.59

Table S2 Calculated results of R_{ct} for different modified electrodes

Electrode	R_{ct}/Ω
GCE (a)	107.0
ABTS/CHIT/GCE (b)	134.2
UiO-66-NH_2/ABTS/CHIT/GCE (c)	143.2
MCS@UIO-66-NH_2/ABTS/CHIT/GCE (d)	104.4
Lac/ABTS/CHIT/GCE (e)	286.8
MCS@UIO-66-NH_2/Lac/ABTS/CHIT/GCE (f)	158.8

Table S3 Performance of the MCS@UIO-66-NH_2/Lac/ABTS/CHIT/GCE tetracycline biosensor compared with those reported TC sensors in literature.

Electrode	Methods	LOD (nM)	Linear range (mol $L^{-1}\times10^{-5}$)	Reference
Pb-PFGE	electrochemical	4.0	0.005 –1.0	S10
GO/MWCNT-COOH/CPE	electrochemical	360	2.0 –31.0	S11
Au/g-C_3N_4/GCE	electrochemical	300	0.01–20.0	S12
CB-PS/GCE	electrochemical	1150	0.5–12.0	S13
PEI/$TetX_2$/npGCE	electrochemical	180	0.05–0.5	S14
MCS@UiO-66-NH_2/Lac/ABTS/CHIT/GCE	Electrochemical enzymatic	894	0.1–6.0	This work

PFGE: polymer filmed glassy carbon electrode; MWCNTs: multiwall carbon tubes; GCE: glassy carbon electrode; GO: graphene oxide; CPE: carbon paste electrode; g-C_3N_4: graphitic carbon nitride; CB-PS: carbon black-potato starch biopolymer; PEI: poly- ethyleneimine; $TetX_2$: $TetX_2$ monooxygenase; npGCE: nano porous glassy carbon electrode

References

S1 M. Fabbrini, C. Galli and P. Gentili, J. Mol. Catal. B Enzym., 2002, **16**, 231–240.

S2 H. Xie, J. Chong, Y. Tian and X. Wang, *J. Porous Mater.,* 2019, **26**, 185–191.

S3 X. Xiao, B. Han, G. Chen, L. Wang and Y. Wang, *Sci. Rep*., 2017, **7**, 40167.

S4 A. Kołodziejczak-Radzimska, A. Budna, F. Ciesielczyk, D. Moszyński and T. Jesionowski, *Process Biochem*., 2020, **95**, 71–80.

S5 J. H. Cavka, S. Jakobsen, U. Olsbye, N. Guillou, C. Lamberti, S. Bordiga, K. P. Lillerud, *J. Am. Chem. Soc.*, 2008, **130**, 13850–13851.

S6 X. Luo, C. Wang, L. Wang, F. Deng, S. Luo, X. Tu and C. Au, *Chem. Eng. J*., 2013, **220**, 98–

106.

S7 F. Aghili, A.A. Ghoreyshi, A. Rahimpour and B. V. D. Bruggen, *Ind. Eng. Chem. Res*., 2020, **59**, 7825–7838.

S8 Y. Liu, Z. Zeng, G. Zeng, L. Tang, Y. Pang, Z. Li, C. Liu, X. Lei, M. Wu, P. Ren, Z. Liu, M. Chen and G. Xie, *Bioresour. Technol.*, 2012, **115**, 21–26.

S9 C. Chao, J. Liu, J. Wang, Y. Zhang, B. Zhang, Y. Zhang, X. Xiang and R. Chen, *ACS Appl. Mater. Inter.*, 2013, **5**, 10559–10564.

S10 Z. Rajab Dizavandi, A. Aliakbar and M. Sheykhan, *Electrochim. Acta*, 2017, **227**, 345–356.

S11 A. Wong, M. Scontri, E. M. Materon, M. R. V Lanza and M. D. P. T. Sotomayor, J. *Electroanal. Chem.*, 2015, **757**, 250–257.

S12 H. Guo, Y. Su, Y. Shen, Y. Long and W. Li, *J. Colloid Interface Sci.*, 2019, 536, 646–654.

S13 K. P. Delgado, P. A. Raymundo-Pereira, A. M.Campos, O. N. O. Jr and B. C. Janegitz, *Electroanal*. 2018, **30**, 2153-2159.

S14 M. Besharati, J. Hamedi, S. Hosseinkhani and R.Saber, *Bioelectrochem.*, 2019, **128**, 66-73.